

# A Tactile Sensor Instantaneously Evaluating Friction Coefficients

Katsuhiko Nakamura\* and Hiroyuki Shinoda\*\*

\*Tokyo Univ. of Agriculture & Technology, 2-24-16 Koganei, Tokyo 184-8588 Japan

\*\*The Univ. of Tokyo, 7-3-1 Hongo, Bunkyo-ku, Tokyo 113-0033 Japan

shino@alab.t.u-tokyo.ac.jp

## SUMMARY

A human can lift up an object with the almost minimum grasping force regardless of the friction coefficient between the fingers and the object, but the sensing mechanism for this remarkable task has not been well explicated yet. Last year we proposed a tactile sensing principle to detect a friction coefficient at the moment of touching. But we have not confirmed that principle with a real sensor yet. In this paper we propose a structure of the sensor and show successful results of friction coefficient detection.

**Keywords:** tactile Sensor, haptic interface, friction coefficient, grasping.

## INTRODUCTION

It is known that a human can lift up an object with almost minimum grasping force regardless of the friction coefficient between the fingers and the object [1], but the sensing mechanism for this remarkable task has not been well explicated yet. One strategy to mimic this task in robotics is pre-perception of the friction coefficient by rubbing an object with the finger before grasping. Another approach is detecting dynamic signals [2] arising at slip outsets.

Meanwhile we proposed a tactile sensor that detects friction coefficients at the moment of touching [3]. We showed a theory and calculation results that suggest sensing vertical and horizontal stress in a sensor skin simultaneously, gives the friction coefficient between the sensor and an object without any preliminary motions. But we had not confirmed that principle using a real sensor yet. In this paper we propose a structure of the sensor using ARTC tactile sensing element [4] and show successful results of friction coefficient detection. Using this sensor we will easily realize the “minimal force grasping” simply by gradually increasing both the grip force and lift force according to the sensor signal.

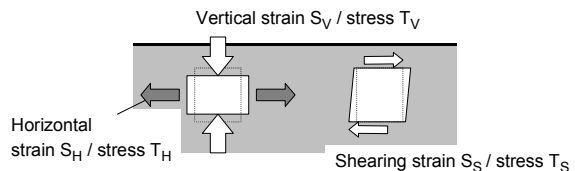


**Fig. 1:** The terminology of strain component in this paper. We call normal strain/stress component along the surface “horizontal strain/stress,” while we simply call normal strain/stress vertical to the surface “Vertical strain/stress.”

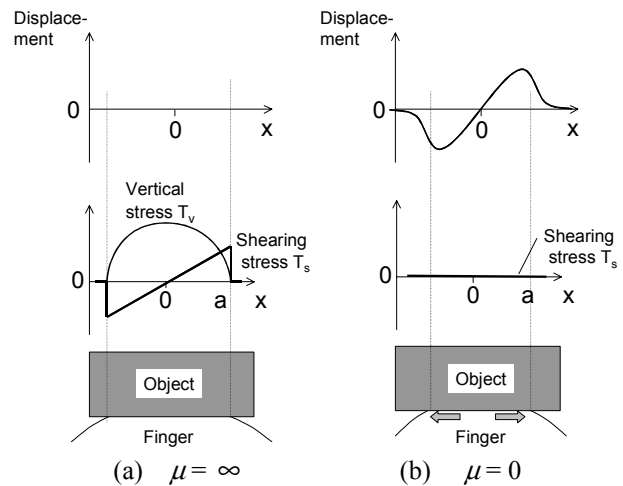


**Fig. 2:** Deformation and shearing stress when a finger (tactile sensor) touches an object vertically.

## SENSING PRINCIPLE

Suppose a tactile sensor has a sensing element that detects both vertical and horizontal strain. See Fig. 1. When a rigid object is pressed on the sensor as shown in Fig. 2, the deformation of the sensor under the contact area depends on the friction coefficient.

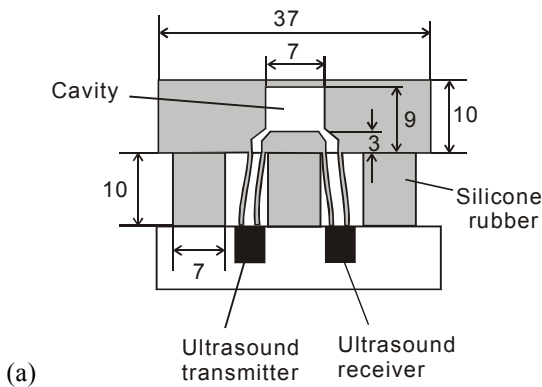
**Case 1:** If the friction coefficient is zero, the sensor skin extends horizontally, and small slips arise overall the contact area. See Fig.2 (b).

**Case 2:** If the friction coefficient is sufficiently large, the skin can not move horizontally, and a shearing stress distribution  $T_s(x)$  arises as shown in Fig. 2 (a).

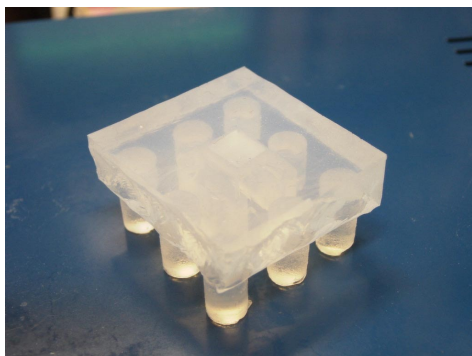
FEM results for finite friction coefficients  $\mu$ , shows horizontal stress under the surface changes continuously as the  $\mu$  changes [3] unless  $\mu$  is much larger than 1. Therefore if we sense the horizontal stress under a contact area, we can estimate the friction coefficient.

### STRUCTURE OF THE SENSOR

Fig. 3 shows the structure of the sensor. An elastic body has a tactile sensing element called “Acoustic Resonant Tensor Cell” (ARTC) [4]. The ARTC is a parallelepiped cavity connected to an ultrasound transmitter and receiver. From the three primary acoustic resonant frequencies of the cavity air, it detects the extension of the cavity along the edges. The skin is sustained by nine projections as the figure shows in order to make the horizontal constraint under the skin free.



(a)



(b)

**Fig. 3:** Structure of the sensor with an ARTC. The sensor body is made of transparent silicone rubber.

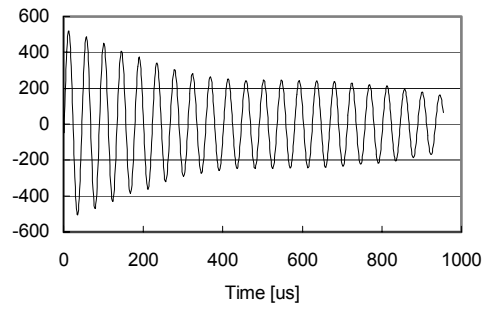


**Fig. 4:** Relaxation signal of the 22.5 kHz  $f_1$  mode.

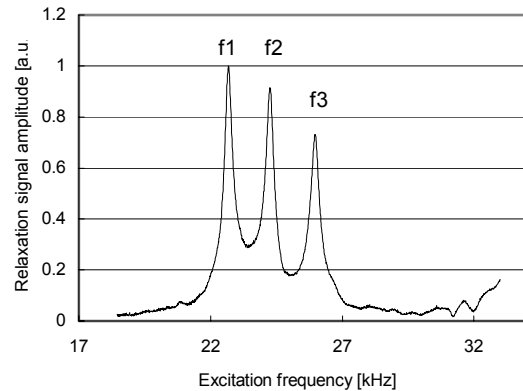


**Fig. 5:** Three primary resonant frequencies  $f_1$ ,  $f_2$ , and  $f_3$  corresponding to the three edges of the parallelepiped.  $f_1$  and  $f_2$  are those of the horizontal modes, and  $f_3$  the vertical mode.

### RESONANT FREQUENCY DETECTION

After stopping a burst signal from the ultrasound transmitter that excites the cavity air, we observe a relaxation signal as shown in Fig. 4 at the ultrasound receiver when the excitation frequency is close to the resonant frequencies. The frequency of the relaxation signal is always equal to the resonant frequency of the cavity air regardless of the excitation frequency while the amplitude depends on the excitation frequency.

Fig. 5 shows the amplitude of the relaxation signal versus the excitation frequency. The excitation signals are 2 ms burst with constant amplitude. Three peaks corresponding to the three primary resonant modes are seen. The three frequencies indicate the lengths of the three edges of the parallelepiped cavity. We estimate the vertical cavity extension ratio  $u_V$  as

$$u_V = -\frac{\Delta f_3}{f_3} \quad (1)$$

and the horizontal cavity extension ratio along one (of two) direction  $u_H$  as

$$u_H = -\frac{\Delta f_1}{f_1} \quad (2)$$

The sampling of the tactile signal is done as follows. We excite the cavity air at the measured resonant frequency in the former sampling. A computer calculates the frequency of the relaxation signal after AD converting. This process is done three times sequentially for the three resonant modes. Sampling time (the time to obtain all three frequencies) in the current system is 0.39 sec. Theoretically the minimum sampling time to obtain one resonant frequency is several millisecond that is the duration of the relaxation signal.

## EXPERIMENTAL RESULTS

**Fig. 7** shows the measured extensions  $u_H$  and  $u_V$  of the ARTC cavity when three kinds of objects are pressed on the sensor vertically. All the three objects have flat and rigid surfaces, but they are given different frictional properties by covering the surfaces with a sandpaper, powder, and oil, respectively. The characteristics of the friction are shown in **Fig. 6**.

The horizontal extension of the cavity  $u_H$  derived from the resonant frequency  $f_1$ , clearly depends on the friction coefficient. Next we evaluate the influences of contact speed, contact angle, and surface curvature on the friction estimation.

As is seen in **Fig. 7**, the horizontal/vertical cavity extension is proportional to the contact depth. Therefore the ratio

$$R = u_V / u_H \quad (3)$$

is independent of the contact depth. Then we observed the ratio  $R$  in various contact motions for the three kinds of objects. **Fig. 10** shows plots of  $R$  when we pressed the sensor at three kinds of speed 0.8, 0.38, and 0.18 mm/s, respectively. The three motions are illustrated in **Fig. 9** by the measured  $u_V$  in the contact motions. The maximum contact depth was 3 mm that corresponded to  $u_V = -0.12$ . The experimental results in **Fig. 10** showed the three types of frictional properties were distinguishable from  $R$  regardless of the pressing speed.

**Fig. 11** shows plots of  $R$  for inclined oiled surfaces. This figure shows the sensor output is not very sensitive to the inclination of the object surface. **Fig. 12** shows  $R$ s for a curved oiled surface with a curvature radius 10 cm. The difference from the  $R$ s of a flat one decreased as the contact became deep. These results show it is possible to estimate the friction coefficient  $\mu$  from the horizontal and vertical extension of the ARTC cavity when  $\mu$  is smaller than 1.

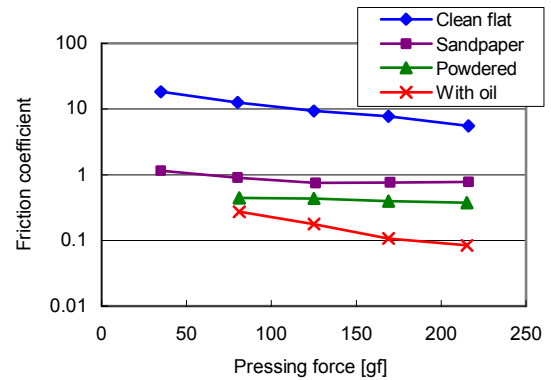
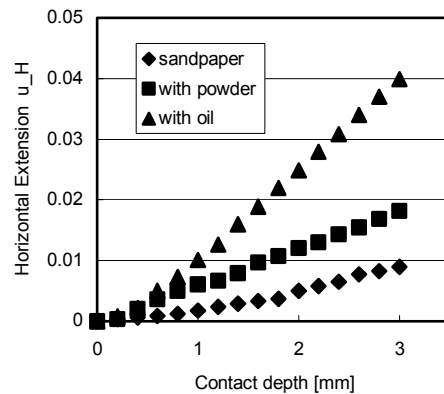
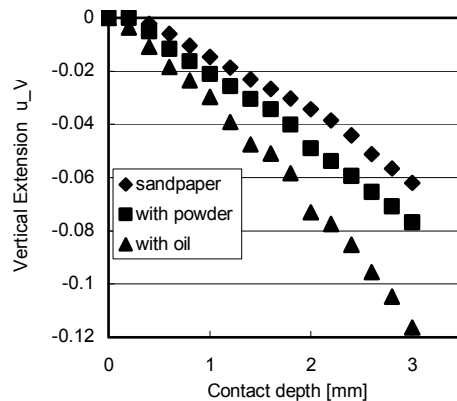


**Fig. 6:** Friction coefficients versus vertical contact force. The friction coefficients between the sensor and hard flat objects covered with a sandpaper, powder and oil were, respectively, about 0.8, 0.4, and 0.1 when the applied contact force to the sensor was 100 gf ~ 200 gf.



(a)



(b)

**Fig. 7:** Measured extension  $u_H$  and  $u_V$  of the cavity when we pressed the sensor with various surfaces. (a): horizontal extension ratio  $u_H$  calculated by Eq. (2), and (b): vertical extension ratio  $u_V$ .

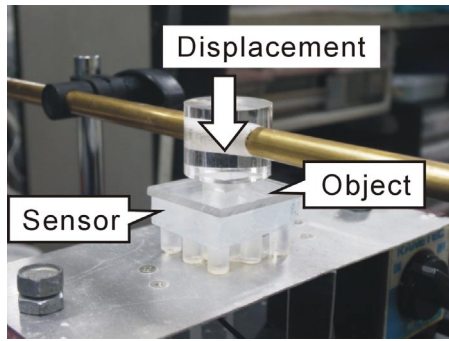


Fig. 8: View of the experiment.

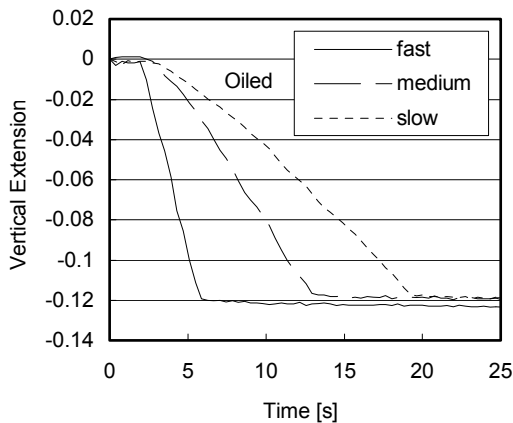


Fig. 9: Vertical extension  $u_V$  for three types of (vertical) contact speeds fast (0.8 mm/s), medium (0.38 mm/s) and slow (0.18 mm/s), respectively.

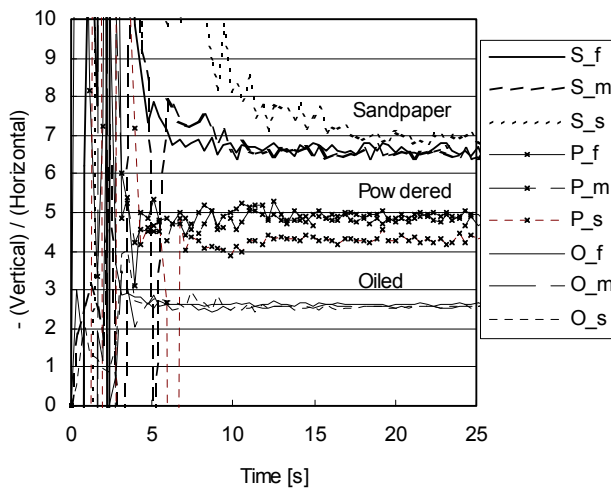


Fig. 10: Plots of  $R$  in Eq. (3) for various objects and contact speeds. The capital letters S, P, and O mean the object surfaces covered with a sandpapers, powder, and oil, respectively. The small letters f, m, and s mean the contact speed fast (0.8 mm/s), medium (0.38 mm/s), and slow (0.18 mm/s), respectively.

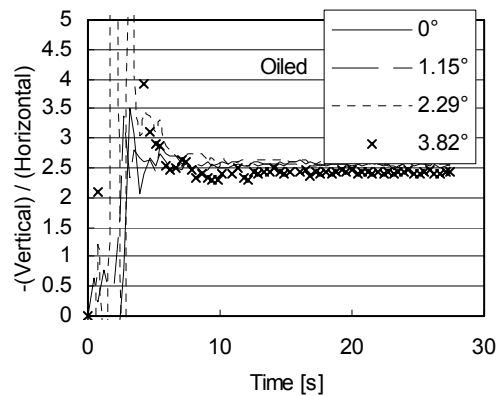


Fig. 11: Plots of  $R$  for inclined oiled surfaces.

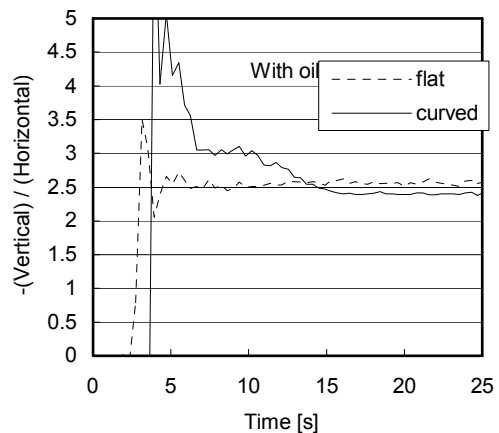


Fig. 12: Comparison between  $R$ s for a curved oiled surface and those for a flat one.

## References

- [1] R.S. Johansson and G. Westling, "Roles of Glabrous Skin Receptors and Sensorimotor Memory in Automatic Control of Precision Grip when Lifting Rougher or More Slippery Objects," *Exp. Brain Res.*, 56, pp.550-564, 1984.
- [2] M. R. Tremblay and M. R. Cutkosky, "Estimating Friction Using Incipient Slip Sensing During a Manipulation Task," *Proc. 1993 IEEE Int. Conf. on Robotics & Automation*, pp. 429-434, 1993.
- [3] H. Shinoda, S. Sasaki, and K. Nakamura, "Instantaneous Evaluation of Friction Based on ARTC Tactile Sensor," *Proc. 2000 IEEE Int. Conf. on Robotics and Automation*, pp.2173-2178, 2000.
- [4] H. Shinoda, K. Matsumoto and S. Ando, "Tactile Sensing Based on Acoustic Resonance Tensor Cell," *Proc. TRANSDUCERS '97, Vol. 1*, pp. 129-132, 1997.